

## **An Important Biogeochemical Link between Organic and Inorganic Carbon Cycling: Effects of Organic Alkalinity on Carbonate Chemistry in Coastal Waters Influenced by Intertidal Salt Marshes**

Shuzhen Song<sup>a,b</sup>, Zhaohui Aleck Wang<sup>b,\*</sup>, Meagan Eagle Gonnee<sup>c</sup>, Kevin D. Kroeger<sup>c</sup>,  
Sophie N. Chu<sup>d</sup>, Daoji Li<sup>a,\*</sup>, and Haorui Liang<sup>b,e</sup>

<sup>a</sup> State Key Laboratory of Estuarine and Coastal Research, East China Normal University, Shanghai 200241, China

<sup>b</sup> Department of Marine Chemistry and Geochemistry, Woods Hole Oceanographic Institution, Woods Hole, Massachusetts 02543, USA

<sup>c</sup> Woods Hole Coastal and Marine Science Center, U. S. Geological Survey, Woods Hole, Massachusetts 02543, USA

<sup>d</sup> Joint Institute for the Study of the Atmosphere and Ocean, University of Washington, Seattle, Washington 98105, USA

<sup>e</sup> College of Chemistry and Chemical Engineering, Ocean University of China, Qingdao, Shandong 266100, China

\*Corresponding authors.

Email addresses: [zawang@whoi.edu](mailto:zawang@whoi.edu) (Zhaohui Aleck Wang)

[daoji@sklec.ecnu.edu.cn](mailto:daoji@sklec.ecnu.edu.cn) (Daoji Li)

## **Abstract**

Dissolved organic carbon (DOC) contains organic acid charge groups that contribute organic alkalinity (OrgAlk) to total alkalinity (TA). These effects are often ignored or treated as a calculation uncertainty in many aquatic CO<sub>2</sub> studies. This study evaluated OrgAlk variability, sources, and characteristics in estuarine waters exchanged tidally with a groundwater-influenced salt marsh in the northeast USA. OrgAlk provided a biogeochemical link between organic and inorganic carbon cycling through its direct effects on pH, and thus CO<sub>2</sub> system speciation and buffer capacity. Two main charge groups were identified including carboxylic and phenolic or amine groups. Terrestrial groundwater and in-situ production within salt marsh peat contributed OrgAlk to the tidal creek, with the former being a more significant source. Groundwater entering the marsh complex contained exceptionally high OrgAlk (> 150 μmol kg<sup>-1</sup>), and these compounds were preferentially preserved within the DOC pool during groundwater transport and mixing with coastal water. OrgAlk:DOC ratios in groundwater and marsh-influenced water varied across space and time. This highlights the insufficiency of using a fixed proportion of DOC to account for organic acid charge groups. Accounting for OrgAlk altered H<sup>+</sup> concentrations by ~ 1 – 41 nmol kg<sup>-1</sup> (equivalent to a pH change of ~ 0.03 – 0.26), pCO<sub>2</sub> by ~ 30 – 1600 μatm and buffer capacity by ~ 0.00 – 0.14 mmol kg<sup>-1</sup> at the relative OrgAlk contributions of 0.9 – 4.3% of TA observed in the marsh-influenced tidal water. Thus, OrgAlk may have a significant influence on coastal inorganic carbon cycling. Further theoretical calculations confirm that these concentrations of OrgAlk would have sizable impacts on both carbonate speciation and, ultimately, air-sea CO<sub>2</sub> fluxes in different coastal environments, ranging from estuarine to shelf waters. A new conceptual model linking organic and inorganic carbon cycling for coastal waters is proposed to highlight the sources and sinks of organic acid charge groups, as well as their biogeochemical behaviors and mechanistic control on the CO<sub>2</sub> system.

*Keywords* : Organic alkalinity; Carbon dioxide; Carbon cycle; Salt marsh; Groundwater; Coastal ocean

# 1 1. Introduction

2  
3 Highly productive coastal salt marshes contain large carbon stocks with high rates of  
4 storage ( $18 - 1713 \text{ g C m}^{-2} \text{ yr}^{-1}$ ), and thus play an important role in the coastal carbon cycle  
5 (Bauer et al., 2013; Ouyang and Lee, 2014; Holmquist et al., 2018; Najjar et al., 2018).  
6 These ecosystems export large quantities of dissolved inorganic carbon (DIC), total  
7 alkalinity (TA), and dissolved organic carbon (DOC) to nearby marine systems via tidal  
8 exchange (Downing et al., 2009; Wang et al., 2016; Chu et al., 2018), although current  
9 estimates of these lateral fluxes still bear large uncertainties (Cai, 2011; Bauer et al., 2013;  
10 Najjar et al., 2018). Export of DIC and TA from these coastal vegetated ecosystems  
11 significantly affects the carbonate system in adjacent coastal waters (Raymond et al., 2000;  
12 Wang and Cai, 2004; Wang et al., 2016).

13 In both freshwater and seawater, DOC contributions to TA, i.e. organic alkalinity (OrgAlk),  
14 affect water pH, carbonate speciation, and buffer capacity (e.g., Cai et al., 1998; Muller and  
15 Bleie, 2008; Wang et al., 2013; Wang et al., 2016). Since salt marshes export DOC produced  
16 during marsh metabolic processes, elevating DOC in marsh-influenced coastal waters,  
17 OrgAlk could be a significant component of TA at these sites. Nevertheless, assessment of  
18 OrgAlk content and potential effects in estuarine waters adjacent to salt marshes is lacking.

19 In natural water, TA is defined as the excess of proton acceptors (bases formed from weak  
20 acids with a dissociation constant  $K \leq 10^{-4.5}$ , corresponding to that of carbonic acid) over  
21 proton donors (acids with  $K > 10^{-4.5}$ ) (modified from Dickson, 1981):

$$\begin{aligned} \text{TA} = & [\text{HCO}_3^-] + 2[\text{CO}_3^{2-}] + [\text{B}(\text{OH})_4^-] + [\text{HPO}_4^{2-}] + 2[\text{PO}_4^{3-}] + [\text{SiO}(\text{OH})_3^-] \\ & + [\text{HS}^-] + [\text{NH}_3] + [\text{OrgAlk}] + [\text{OH}^-] - [\text{H}^+]_{\text{F}} - [\text{HF}] - [\text{HSO}_4^-] \\ & - [\text{H}_3\text{PO}_4] - [\text{OrgA}] \dots, \end{aligned} \quad (1)$$

22 where contributions of carbonate ( $\text{HCO}_3^-$  and  $\text{CO}_3^{2-}$ ) and borate ( $\text{B}(\text{OH})_4^-$ ) species usually  
23 dominate. Organic acid charge groups (negatively charged species) can contribute to TA as a  
24 base (OrgAlk) and/or an acid (OrgA) depending on their equilibrium constants (Muller and  
25 Bleie, 2008; Ulfsbo et al., 2015). Since TA is commonly used as one input parameter in  
26 thermodynamic  $\text{CO}_2$  system calculations, any uncertainty in the definition of TA will lead to  
27 uncertainty in determining carbonate speciation.

28 Organic acid charge groups are often perceived as minor species in natural waters and are  
29 commonly omitted during  $\text{CO}_2$  system speciation calculations (e.g., Kaltin and Anderson,  
30 2005; Paquay et al., 2007; Butman and Raymond, 2011). Nevertheless, previous studies  
31 have shown that OrgAlk can be a significant portion of TA in organic carbon-rich waters  
32 such as humic-rich rivers and coastal waters, with concentrations varying from negligible to

33 over  $100 \mu\text{mol kg}^{-1}$  (Cai et al., 1998; Hernández-Ayon et al., 2007; Muller and Bleie, 2008;  
34 Kim and Lee, 2009; Wang et al., 2013; Kuliński et al., 2014; Yang et al., 2015; Ko et al.,  
35 2016; Hammer et al., 2017). The reported effect of ignoring OrgAlk in  $\text{CO}_2$  calculations can

36 range from 10 – 60% underestimation to > 160% overestimation of  $p\text{CO}_2$  depending on  
37 whether the TA-DIC or TA-pH pair is used (Tishchenko et al., 2006; Hunt et al., 2011;  
38 Koeve and Oschlies, 2012; Wang et al., 2013; Kuliński et al., 2014; Abril et al., 2015; Yang  
39 et al., 2015). Moreover, the impact of OrgAlk extends beyond a source of calculation  
40 uncertainty in the  $\text{CO}_2$  system. The biogeochemical cycling of organic acid charge groups  
41 directly impacts water pH, and thus carbonate speciation, which may ultimately influence  
42 air-water  $\text{CO}_2$  exchange and inorganic carbon fluxes (e.g., lateral transport and upwelling).  
43 Therefore, we propose that the effects of OrgAlk on the  $\text{CO}_2$  system may represent an  
44 important biogeochemical linkage between organic and inorganic carbon cycling, especially  
45 in organic carbon-rich waters.

46 Herein, we present the first study of OrgAlk in tidal water exchanged between an  
47 estuary and a salt marsh system. The goal was to investigate OrgAlk as a biogeochemical  
48 linkage between organic and inorganic carbon cycling by studying the sources and  
49 composition of OrgAlk, and quantitatively assessing its impacts on the  $\text{CO}_2$  system in  
50 marsh-influenced coastal water. A simple titration model was used to identify the charge  
51 groups of organic acids. The effect of OrgAlk on the  $\text{CO}_2$  system speciation and coastal  
52 ocean buffer capacity was assessed by including OrgAlk within the traditional seawater  $\text{CO}_2$   
53 system calculations. Finally, a conceptual model, depicting the generation and removal of  
54 organic acid charge groups within the DOC pool, provides insights into the biogeochemical  
55 regulation of the aquatic  $\text{CO}_2$  system through OrgAlk contributions.

56

## 57 **2. Method**

58

### 59 **2.1 Study site**

60

61 Sage Lot Pond (SLP) is an intertidal salt marsh, with minimal human impact and nitrogen  
62 loading, located on the eastern side of Waquoit Bay (Fig. 1a and 1b), a shallow estuary on  
63 the south coast of Cape Cod, Massachusetts, U.S.A. Groundwater (GW) discharge is the  
64 main form of freshwater input to the coast due to highly permeable glacial sand deposits in  
65 the region (Cambareri and Eichner, 1998). The annual flux of GW to the SLP tidal creek,  
66 where this study was conducted, is about  $6310 \text{ m}^3$  or 0.3% of the mean annual tidal  
67 exchange (Wang et al., 2016). The plant community in the SLP marsh is dominated by  
68 *Spartina patens*, *Distichlis spicata*, and *Juncus gerardii* in the high marsh and *Spartina*  
69 *alterniflora* in the low marsh (Moseman-Valtierra et al., 2016) (Fig. 1c). The SLP watershed  
70 is forested with a mixture of pitch pine and scrub oak (Fig. 1d).

71

### 72 **2.2 Sampling and measurements**

73

74 The entrance to the SLP tidal creek was instrumented with a YSI EXO2 Sonde (YSI Inc.,  
75 Ohio, USA) to collect in-situ physical parameters including temperature and water depth  
76 (Fig. 1d) (Mann et al., 2019). Time-series bottle samples for TA, DIC, OrgAlk, pH, and  
77 DOC were collected hourly at ~ 0.2 m below the surface at the creek mouth over several

78 tidal cycles in May, July, October, and November 2016. The water elevation at the sampling  
79 site varied between -0.25 m and 0.64 m (North American Vertical Datum of 1988 or  
80 NAVD88), and the water column was well-mixed. Samples for practical salinity (Sp) were  
81 collected and analyzed with a Guideline AutoSal instrument at Woods Hole Oceanographic  
82 Institution (WHOI). GW was sampled on September 16<sup>th</sup>, 2016 from a push point sampler  
83 installed within the forest adjacent to the marsh at 0.56 m, 0.89 m, and 1.8 m below the land  
84 surface to collect OrgAlk, TA, pH, and DOC samples. GW salinity and temperature were  
85 measured with a YSI Pro30 (YSI Inc., Ohio, USA) during collection. To constrain the  
86 coastal water OrgAlk endmember, two OrgAlk, TA, and pH samples were collected from  
87 the WHOI Environmental Systems Laboratory intake, located about 1.6 km offshore in  
88 Vineyard Sound (orange square in Fig. 1a), on March 8<sup>th</sup> and July 9<sup>th</sup>, 2018, and one DOC  
89 sample was collected on March 8<sup>th</sup>, 2018.

90 The TA, DIC, and pH sample collection protocol was based on the best practices of  
91 seawater CO<sub>2</sub> measurements outlined in Dickson et al. (2007). OrgAlk sample collection  
92 followed the TA sampling protocol. In brief, water samples were pumped through 0.45 μm  
93 air-tight capsule filters (Farr West Environmental Supply, Texas, USA) and collected into  
94 250 mL borosilicate glass bottles for TA, DIC, pH, and OrgAlk measurements. All samples  
95 were filtered to remove particles from the turbid coastal water. These particles interfere with  
96 TA, DIC, and pH measurements in several ways, including clogging analytical instruments,  
97 interfering with spectrophotometric analyses, and potential inclusion of solid carbonate  
98 minerals within the samples. Previous experience indicates that the pressure change that  
99 occurs due to our filtering procedure is not likely to change the TA, DIC, and pH values of a  
100 sample. Each sample was preserved with 100 μL of a saturated mercuric chloride solution.  
101 Samples for DOC analysis were filtered through 0.45 μm pore size polyethersulfone  
102 cartridge filters into combusted borosilicate glass vials with Teflon-lined silicone septa caps,  
103 acidified to pH < 2 with hydrochloric acid and refrigerated until analysis.

104 DIC samples were measured with a DIC auto-analyzer (AS-C3, Apollo SciTech Inc.,  
105 Delaware, USA). Each sample was acidified with 10% phosphoric acid and purged with  
106 high purity N<sub>2</sub> gas, and the evolved CO<sub>2</sub> gas was detected and quantified by a LiCOR7000  
107 infrared CO<sub>2</sub> analyzer (LI-COR Environmental, Nebraska, USA). A certified reference  
108 material (CRM) from Dr. A. G. Dickson at the Scripps Institution of Oceanography was  
109 used for calibration. The precision and accuracy of DIC measurements were both ± 2.0  
110 μmol kg<sup>-1</sup>.

111 The pH samples were measured with a UV-visible spectrophotometer (Agilent 8454,  
112 Agilent Technologies, USA) at 25 ± 0.1°C using purified meta-cresol purple (mcp) as an  
113 indicator. The mcp model reported in Douglas and Byrne (2017) was applied to calculate  
114 pH across the salinity and temperature ranges in this study. The pH values are reported on  
115 the total proton concentration scale and converted from 25 ± 0.1°C to in-situ temperature  
116 using measured DIC and the CO2SYS program (van Heuven et al., 2011). The mean  
117 uncertainty of the pH measurement was ± 0.006 (range 0.0003 – 0.017), calculated as the  
118 mean difference between duplicate samples (n = 40). The difference between pH values of  
119 duplicate samples were much higher in samples collected in May and July (mean: 0.007,

120 range: 0.0003 – 0.017) than those collected in October and November (mean: 0.001, range:  
121 0.0007 – 0.003). This is likely due to the presence of more colored material, potentially  
122 chromophoric dissolved organic matter, and particles smaller than 0.45  $\mu\text{m}$  in May and July  
123 samples than the October and November samples that were much clearer. Fine particles and  
124 colored material may significantly reduce the accuracy of spectrophotometric pH  
125 measurements, and thus affect  $\text{CO}_2$  calculation accuracy when pH is used as an input  
126 parameter. Alternatively, for future studies in turbid waters (where  $\text{Sp} > 5$ ), sample pH can  
127 be measured potentiometrically on the NIST/NBS scale and converted to the total proton  
128 concentration scale based on the response of the electrode to TRIS buffer solutions prepared  
129 in artificial seawater with similar ionic strengths as the samples (Dinauer and Mucci, 2017).  
130 All TA titrations were conducted at  $22.4 \pm 0.1^\circ\text{C}$  using a ROSS<sup>TM</sup> combination pH electrode.  
131 The electrode was calibrated using three buffer solutions on the National Bureau of  
132 Standard (NBS) scale (pH = 4.01, 7.00, and 10.01). TA was titrated with a dilute  
133 hydrochloric acid (HCl) solution ( $\sim 0.1$  M in 0.7 M NaCl solution) according to a modified  
134 Gran titration procedure (Wang and Cai, 2004) using two digital syringe pumps (Kloehn  
135 Inc., Las Vegas, USA). HCl concentration was calibrated with the CRM. The mean  
136 difference between duplicate samples ( $n = 30$ ) was  $2.5 \pm 1.9$  (one standard deviation)  $\mu\text{mol}$   
137  $\text{kg}^{-1}$ .

138 OrgAlk concentration was determined with the same electrode and digital syringe pumps as  
139 the TA measurements, based on the procedure reported in Cai et al. (1998) (Fig. 2). Briefly,  
140 a 35 g water sample was titrated with a calibrated HCl solution ( $\sim 0.1$  M) until the sample  
141 pH was below 3.0 (first titration).  $\text{CO}_2$  in the sample was then removed by bubbling with  
142 high purity  $\text{N}_2$  gas (99.999%) for  $\sim 10$  minutes. The acidified sample was then titrated with  
143 0.1 M NaOH solution back to its initial pH (back titration). The NaOH solution was  
144 prepared in DI water bubbled with high purity  $\text{N}_2$  gas to prevent  $\text{CO}_2$  dissolution into the  
145 solution. Finally, the sample was titrated with HCl again until its pH was below 3.0 (second  
146 titration). During the back titration and second titration, the titration vessel was covered by a  
147 plastic bag and continuously flushed with  $\text{N}_2$  to maintain a  $\text{CO}_2$ -free environment. In total, 8  
148 – 12 points were acquired for the modified Gran titration between 3.0 – 3.8 pH during the  
149 second titration. OrgAlk was calculated as the TA from the second titration minus the borate  
150 alkalinity. Borate alkalinity was calculated from salinity, temperature, and sample pH on the  
151 NBS scale (Dickson, 1990a; Lee et al., 2010). The mean difference of OrgAlk  
152 concentrations between duplicate samples was  $2.8 \pm 2.1$   $\mu\text{mol kg}^{-1}$  ( $n = 17$ ). The total  
153 concentrations of sulfide in two low tide water samples in April 2019 were 0 – 2  $\mu\text{mol kg}^{-1}$ ,  
154 accounting for 0 – 1  $\mu\text{mol kg}^{-1}$  sulfide alkalinity. Moreover, sulfide alkalinity could be  
155 removed in the form of  $\text{H}_2\text{S}$  along with  $\text{CO}_2$  by  $\text{N}_2$  bubbling after the first titration. Sulfide  
156 alkalinity was thus assumed to be negligible in OrgAlk calculations. Based on nutrient  
157 concentration measurements, the contributions of phosphate, ammonium, and silicate to TA  
158 were  $< 1.0$   $\mu\text{mol kg}^{-1}$  (Supplementary Data A1) and therefore not considered in OrgAlk  
159 calculations.

160 Even though the NaOH solution was prepared under a  $\text{N}_2$ -flushed environment,  $\text{CO}_2$  may  
161 have dissolved into the solution. To determine the residual  $\text{CO}_2$  (in the form of  $\text{CO}_3^{2-}$ ),

162 artificial seawater was prepared according to the recipe of Dickson et al. (2007) while  
 163 excluding bicarbonate/carbonate salts, followed by bubbling with high purity N<sub>2</sub> gas for 4  
 164 hours. The carbonate-free artificial seawater was titrated in a similar procedure as OrgAlk.  
 165 The carbonate ion concentration was calculated as the difference in TA between the first and  
 166 second titration. The results show that there was  $\sim 1.5 \pm 0.2 \text{ mmol L}^{-1} \text{ CO}_3^{2-}$  (n = 11) in the  
 167 NaOH solution ( $\sim 0.1 \text{ M}$ ). The OrgAlk results were corrected by subtracting introduced  
 168 carbonate alkalinity based on the volume of NaOH solution added during the back titration.  
 169 For marsh tidal water and Vineyard Sound coastal water samples, there was  $12 - 17 \text{ } \mu\text{mol}$   
 170  $\text{kg}^{-1}$  carbonate alkalinity introduced by the NaOH solution, compared to  $21 - 31 \text{ } \mu\text{mol kg}^{-1}$   
 171 in GW. The  $\text{CO}_3^{2-}$  concentration in the NaOH solution measured in this study was similar to  
 172 that reported by Yang et al. (2015). Although the low ionic strength of the NaOH solution  
 173 could lead to uncertainties in the determination of OrgAlk in tidal water samples (Sp = 22.8  
 174 – 32.2), we expect this effect to be rather small, as the addition of NaOH solution (214 –  
 175 253  $\mu\text{L}$ ) only changed the sample's ionic strength by 0.6 – 0.7%.

176 To determine OrgAlk composition in different seasons and end-members, full titrations  
 177 were also conducted on one or more tidal water samples from each time-series event  
 178 (excluding October 18<sup>th</sup>), a GW sample (depth = 0.89 m) and a Vineyard Sound coastal  
 179 water sample taken  $\sim 1 \text{ m}$  above the bottom. During a full titration, each sample was first  
 180 titrated to  $\text{pH} < 3.0$ , then bubbled with N<sub>2</sub> gas to remove CO<sub>2</sub>. Thereafter, the sample was  
 181 back titrated to  $\text{pH} > 10.0$  with  $\sim 200$  incremental additions of NaOH (0.1 M) at  $\sim 1 \text{ min}$   
 182 intervals over 3 hours.

183 DOC samples were analyzed on an O. I. Analytical Aurora 1030C Autoanalyzer by  
 184 high-temperature catalytic oxidation followed by nondispersive infrared detection  
 185 (HTCO-NDIR). Concentrations are reported relative to a potassium hydrogen phthalate  
 186 (KHP) standard. Hansell deep seawater (University of Miami Hansell Laboratory, Lot#  
 187 01-14), and Suwannee River NOM (IHSS, Lot# 2R101N) reference materials were  
 188 analyzed daily as additional checks on precision and accuracy of the analyses. Standards  
 189 and reference materials typically vary by  $< 5\%$  (precision), with a sample detection limit of  
 190  $30 \text{ } \mu\text{mol kg}^{-1}$ .

191

### 192 **2.3 OrgAlk model**

193

194 A simple model derived from charge balance (Eq. (2)) was established to determine  
 195 apparent pK values of charge groups during a full titration, with the assumption that all  
 196 weak organic acids can be characterized by one to three monoprotic weak organic acids (Cai  
 197 et al., 1998). The carbonate alkalinity of the NaOH solution was also included in the charge  
 198 balance equation:

$$V_0 \sum_i \frac{X_{iT}}{1 + \frac{[\text{H}^+]}{K_i}} + \frac{V_0 B_T}{1 + \frac{[\text{H}^+]}{K_B}} + \frac{VC_{\text{TNa}}}{1 + \frac{[\text{H}^+]}{K_{\text{C1}}} + \frac{K_{\text{C2}}}{[\text{H}^+]}} + \frac{2VC_{\text{TNa}}}{1 + \frac{[\text{H}^+]^2}{K_{\text{C1}}K_{\text{C2}}} + \frac{[\text{H}^+]}{K_{\text{C2}}}} -$$

$$(V + V_a)([H^+] - [OH^-]) + V_a C_H^0 - VC_B = 0 \quad (2)$$

199 where  $V_0$  is the volume of the sample;  $V_a$  is the volume of acidified sample after the first  
 200 titration;  $V$  is the total volume of base (NaOH) added during a back titration;  $K_i$ ,  $K_B$ ,  $K_{C1}$ ,  
 201 and  $K_{C2}$  are the dissociation constants of charge group  $i$  of organic acids, boric acid, and  
 202 carbonic acid, respectively.  $X_{iT}$  is the total concentration of charge group  $i$  of organic acids  
 203 ( $X_{iT} = [HX_i] + [X_i^-]$ ),  $B_T$  is the total concentration of borate, and  $C_{TNa}$  is the total  
 204 concentration of carbonate in the NaOH solution.  $C_B$  is the concentration of NaOH,  
 205 determined through titration with CRM calibrated HCl.  $C_H^0$  is the hydrogen ion  
 206 concentration after the first titration.  $K_{C1}$ ,  $K_{C2}$ , and  $K_B$  were calculated using temperature  
 207 and salinity using the parameterizations of Cai and Wang (1998) and Dickson (1990a).  
 208 During the  $\sim 3$  h back titration step of a full titration, some  $CO_2$  introduced by the NaOH  
 209 solution might be lost from the sample to the atmosphere, especially when pH was  $< \sim 6$   
 210 (i.e., below the pK value of the first dissociation constant of carbonic acid). This could  
 211 decrease the DIC concentration in the full titration sample. As a result, using the measured  
 212 carbonate concentration in the NaOH solution ( $\sim 1.5 \text{ mmol L}^{-1}$ , see section 2.2) to estimate  
 213 introduced DIC in the full titration samples might result in an over-correction. Instead, we  
 214 used Eq. (2) to simulate the concentration of  $CO_3^{2-}$  in the NaOH solution ( $C_{TNa}$ ) and the  
 215 corresponding introduced DIC ( $VC_{TNa}$  in Eq. (2)) and carbonate alkalinity (terms 3 and 4 in  
 216 Eq. (2)) that best fit the titration curve. The parameters  $X_{iT}$ ,  $K_i$ ,  $C_H^0$ , and  $C_{TNa}$  were  
 217 determined by fitting the nonlinear Eq. (2) using the Matlab™ function ‘leastsq’  
 218 (MathWorks, Inc., USA). First, initial values of  $K_1$ ,  $X_{1T}$ ,  $C_{TNa}$ , and  $C_H^0$  were determined  
 219 from data below pH 5.0; then  $C_H^0$  was fixed and a nonlinear fit was performed iteratively  
 220 for data below pH  $< \sim 7.5$  to re-determine  $X_{1T}$  and  $K_1$ . Finally,  $C_H^0$ ,  $X_{1T}$ , and  $K_1$  were fixed,  
 221 and the values of  $C_{TNa}$ ,  $X_{2T}$ , and  $K_2$  were constrained using all data. A third organic acid  
 222 charge group was identified, if adding  $X_{3T}$  and  $K_3$  improved the fit. The fitting process was  
 223 considered to be complete when the residual of the fit was less than 0.001 and additional  
 224 charge groups did not improve the fit.

225 Assuming zero ionic strength in the samples might introduce uncertainty to pK values of  
 226 identified organic acid charge groups. Masini et al. (1998) evaluated the magnitude of  
 227 variation in pK values of twelve types of humic acids (pK values 3 – 10) at three ionic  
 228 strengths ( $I = 0.01, 0.1, 1.0 \text{ M}$ ). They reported a maximum pK variation of 0.75 over a range  
 229 of ionic strengths from 0.01 to 1.0 M. The maximum salinity of our full titration sample was  
 230 31.5 ( $I = 0.65 \text{ M}$ ). If we adopt the estimate by Masini et al. (1998), ignoring ionic strength  
 231 would result in a maximum error in pK values of 0.49 (i.e.,  $0.65/(1.0-0.01) \times 0.75$ ), assuming  
 232 the change in the pK value is proportional to the change of ionic strength. We thus used 0.49  
 233 as the maximum uncertainty in pK values of organic acid charge groups due to ignoring  
 234 ionic strength in the uncertainty analysis (see section 2.4).

235

#### 236 **2.4 Evaluation of the effects of OrgAlk on the $CO_2$ system**

237

238 The effect of OrgAlk on the  $CO_2$  system was evaluated by incorporating OrgAlk



239 expressions, including the equilibrium constants of all identified organic acid charge groups  
240 and total concentration of each charge group, into the CO2SYS calculation program (van  
241 Heuven et al., 2011) as follows:  
242

$$\text{OrgAlk} = \sum_i \frac{X_{iT}}{1 + \frac{[H^+]}{K_i}} \quad (3)$$

243 Dissociation constants of carbonic acid, boric acid,  $\text{HSO}_4^-$ , and hydrogen fluoride were  
244 taken from Cai and Wang (1998), Dickson (1990a), Dickson (1990b), and Dickson and  
245 Riley (1979), respectively. The total boric acid concentration was computed from the  
246 equation of Lee et al. (2010). Measured values of TA, DIC, equilibrium constants and total  
247 concentrations of organic acid charge groups were used as input parameters to the CO2SYS  
248 program to calculate the values of  $\text{H}^+$ ,  $p\text{CO}_2$ , and other  $\text{CO}_2$  system parameters; the same  
249 calculation was then repeated, but with the total concentrations of organic acid charge  
250 groups set to zero. The effects of OrgAlk were then estimated as the differences in  $\text{H}^+$   
251 concentrations ( $\Delta\text{H}^+$ ),  $p\text{CO}_2$  ( $\Delta p\text{CO}_2$ ), and other  $\text{CO}_2$  parameters between the two  
252 calculations.

253 In the above calculations, TA and DIC values were fixed while OrgAlk varied. This is  
254 analogous to assuming that all organic acid charge groups are produced by organic acids,  
255 thus their variations will ultimately not change TA (Kuliński et al., 2014), since their  
256 dissociation leads to the production of an equivalent amount of  $\text{H}^+$ . Nevertheless, some  
257 organic acid charge groups might be produced concurrently with other cations (e.g.,  $\text{Ca}^{2+}$ ,  
258  $\text{Cu}^{2+}$ , and  $\text{Na}^+$ ) to maintain charge balance. For example, organic acid charge groups may  
259 cycle with  $\text{Zn}^{2+}$  or  $\text{Cu}^{2+}$  during dissociation/association of metal-humic complexes  
260 (Garcia-Mina, 2006; Shi et al., 2016), resulting in net gain or loss of TA. Given that there is  
261 little knowledge of how organic acid charge groups cycle with  $\text{H}^+$  vs. with other cations, we  
262 do not know the exact magnitude of TA change when organic acid charge groups vary. This  
263 prevents us from resolving the  $\text{CO}_2$  system without proper constraints on TA. Thus, we  
264 calculated the impact of OrgAlk by assuming no change in TA. The explicit calculation of  
265 the OrgAlk effects on the  $\text{CO}_2$  system requires future studies on how these charge groups  
266 are generated and cycled in the aquatic environment. In our scenario (constant TA), OrgAlk  
267 does not have a direct effect on the carbonate alkalinity, but the variation in OrgAlk changes  
268 the  $\text{H}^+$  concentration and, thus, affects carbonate alkalinity.

269 Buffer capacity is a measure of the resistance of a natural water or solution to pH change  
270 following the addition of an acid or base (Morel and Hering, 1993). The traditional buffer  
271 factor ( $\beta_{\text{H}}$ ) can be calculated directly from the buffer factor ( $\beta_{\text{Alk}}$ ) proposed by Egleston et al.  
272 (2010). Organic acid charge groups also provide buffer capacity and affect water pH and  
273 acid-base speciation, thus OrgAlk was added into the buffer capacity equation:  
274

(4)

$$\beta_H = -\left(\frac{\partial \text{pH}}{\partial \text{TA}}\right)^{-1} = -2.3 \beta_{\text{Alk}}$$

275 where,

$$\beta_{\text{Alk}} = \frac{\text{Alk}_c^2}{\text{DIC}} - S \quad (5)$$

$$S = \sum_i \frac{[\text{H}^+][\text{X}_i^-]}{K_i + [\text{H}^+]} + \frac{[\text{H}^+][\text{B}(\text{OH})_4^-]}{K_B + [\text{H}^+]} + [\text{HCO}_3^-] + 4[\text{CO}_3^{2-}] + [\text{H}^+] - [\text{OH}^-] \quad (6)$$

276  $\text{Alk}_c$  and  $\text{X}_i^-$  represent the carbonate alkalinity and organic acid charge group  $i$ , respectively.  
 277 The effect of OrgAlk on the buffer capacity was calculated as the difference between the  
 278 buffer capacity calculated with and without OrgAlk ( $\Delta\beta_H$ ). Note that the change of pH and  
 279 acid-base speciation induced by OrgAlk could also affect the carbonate, borate, and other  
 280 buffer systems in natural water.  $\Delta\beta_H$  thus includes a direct effect of OrgAlk on  $\beta_H$  by  
 281 offering extra buffer capacity and an indirect effect by influencing water pH and other  
 282 buffer systems.

283 The uncertainties of OrgAlk effects on the  $\text{H}^+$  concentration and  $p\text{CO}_2$  were calculated using  
 284 the error propagation program of Orr et al. (2018), modified by adding uncertainties in the  
 285 estimated pK values of organic acid charge groups due to the effect of ionic strength. The  
 286 uncertainties in  $\Delta\beta_H$  were calculated based on a first-order Taylor series expansion,  
 287 accounting for parameter uncertainties derived from the error propagation program and  
 288 measurement uncertainties. The combined uncertainties in  $\Delta\text{H}^+$ ,  $\Delta p\text{CO}_2$ , and  $\Delta\beta_H$  include the  
 289 uncertainties in pK values of organic acid charge groups, carbonic and boric acids, as well  
 290 as DIC, TA, and OrgAlk measurement uncertainties.

291

### 292 3. Results

293

#### 294 3.1 Excess alkalinity versus titrated OrgAlk

295

296 Excess alkalinity ( $\Delta\text{TA}$ ), defined as the difference between measured TA and calculated TA  
 297 using measured DIC and pH as input parameters in CO2SYS, has been used in the past to  
 298 estimate OrgAlk (e.g., Kuliński et al., 2014; Yang et al., 2015; Ko et al., 2016; Hammer et  
 299 al., 2017). In our analysis, pooled titrated OrgAlk and  $\Delta\text{TA}$  data did not show a strong  
 300 statistical relationship (Fig. 3). This may be due to colored material and fine particles (<  
 301 0.45  $\mu\text{m}$ ) in tidal water that interfere with spectrophotometric pH measurements.  
 302 Nevertheless, in October and November,  $\Delta\text{TA}$  and OrgAlk values were similar (mean  $\Delta\text{TA}$ :  
 303  $32 \pm 8 \mu\text{mol kg}^{-1}$ , mean OrgAlk:  $34 \pm 7 \mu\text{mol kg}^{-1}$ ) with the linear slope close to 1,  
 304 compared to May (slope  $\ll 1$ ) and July (slope  $< 1$ ) when more water color and fine  
 305 particles were observed in the samples (Fig. 3). Uncertainties in carbonate system  
 306 calculations, including those in TA and DIC measurements and the dissociation constants of  
 307 carbonic acid (Cai and Wang, 1998), boric acid (Dickson, 1990a),  $\text{HSO}_4^-$  (Dickson, 1990b),  
 308 and hydrogen fluoride (Dickson and Riley, 1979), might also contribute to this discrepancy.  
 309 Further studies are required to examine this difference, which also highlights the importance  
 310 of directly measuring OrgAlk.

311

### 312 **3.2 Tidal and seasonal variability**

313

314 OrgAlk, DOC, TA, pH (total proton concentration scale at in-situ temperature), salinity, and  
315 temperature (T) in the Sage Lot Pond tidal creek in May, July, October, and November  
316 varied over tidal cycles and across all seasons (Fig. 4). pH was generally highest at high tide  
317 and lowest at low tide. Salinity typically varied by  $< 3$  over a tidal cycle. DOC and OrgAlk  
318 showed similar trends over tidal cycles, with concentrations increasing from high to low  
319 tide.

320 In May, the salinity in the salt marsh tidal creek ( $S_P = 22.5 - 29.0$ , Fig. 4a and 4b) was much  
321 lower than in the adjacent coastal water ( $S_P = \sim 32$ ). This low salinity was due to GW input,  
322 since there is no river discharge at the study site. As such, three end-members (GW, salt  
323 marsh, and coastal water) may affect the carbonate chemistry in the tidal water at the study  
324 site. Salinity was higher on May 25<sup>th</sup>, suggesting a greater GW input on May 9<sup>th</sup> (Fig. 4a  
325 and 4b). On May 9<sup>th</sup>, the mean OrgAlk concentration was about  $9 \mu\text{mol kg}^{-1}$  higher than on  
326 May 25<sup>th</sup>, but the mean TA value was about  $180 \mu\text{mol kg}^{-1}$  lower (Fig. 4a and 4b). OrgAlk  
327 and DOC also covaried more strongly on May 9<sup>th</sup> (Fig. 4a).

328 In the summer, salinity was lower on July 12<sup>th</sup> ( $S_P = 27.0 - 30.2$ , Fig. 4c) than on July 26<sup>th</sup>  
329 ( $S_P = 29.7 - 30.5$ , Fig. 4d). In contrast to May, when TA did not show a clear covariation  
330 with tides, TA concentrations in July generally increased from high to low tide, especially  
331 on July 26<sup>th</sup> when TA increased  $> 100 \mu\text{mol kg}^{-1}$  (Fig. 4c and 4d). This is consistent with  
332 previous observations of TA production by anaerobic respiration in tidal marshes (Wang et  
333 al., 2016). DOC was up to  $100 \mu\text{mol kg}^{-1}$  higher at low tide than at high tide in the summer,  
334 similar to the TA trend (Fig. 4c and 4d), indicating in-situ production of DOC in salt  
335 marshes. Interestingly, although DOC concentrations in July were generally higher than in  
336 May, OrgAlk concentrations were lower in July than in May when the influence of GW was  
337 apparent. Meanwhile, OrgAlk concentrations were elevated by  $10 - 20 \mu\text{mol kg}^{-1}$  from high  
338 to low tide in July (Fig. 4c and 4d).

339 In October and November, the influence of GW was even more limited, with salinity  $> 28.8$   
340 (Fig. 4e and 4f). During the fall sampling events, average water elevation was higher than in  
341 spring or summer. TA varied from 1884 to 1998  $\mu\text{mol kg}^{-1}$  over two tidal cycles, generally  
342 lower than in July (Fig. 4). Both DOC and OrgAlk concentrations were the lowest observed  
343 among the three seasons (Fig. 4).

344

### 345 **3.3 Characteristics of organic acid charge groups**

346

347 Apparent pK values and total concentrations of organic acid charge groups in GW, Vineyard  
348 Sound coastal water and tidal waters across three seasons were determined by fitting the  
349 non-linear model (Eq. 2) to the full titration data (Table 1). As an example, the May 25<sup>th</sup> full  
350 titration of sample D is shown in Supplementary Data A2. The simulated concentration of  
351  $\text{CO}_3^{2-}$  in NaOH solution was  $1.2 \text{ mmol L}^{-1}$  on average (range  $0.5 - 1.5 \text{ mmol L}^{-1}$ ). The  
352 estimated pK values of the organic acid charge groups showed a  $0.1 - 0.4$  difference when

353 calculated with and without the carbonate alkalinity from the NaOH solution. Two organic  
354 acid charge groups were identified in all titrated samples. The pK value of charge group 1  
355 ( $pK_1$ ) ranged from 4.1 to 5.5, with the highest value in sample B collected on May 9<sup>th</sup>, and  
356 the lowest value in sample D collected on May 25<sup>th</sup>. Most pK values of charge group 2 ( $pK_2$ )  
357 were in the range of 7.4 – 8.4, except sample A on May 9<sup>th</sup> with a much higher value of 9.8.  
358 Sample A was collected during the same time series as samples B and C at similar salinities  
359 (Table1). The pK values of the two charge groups in samples B (5.5 and 7.4) and C (5.1 and  
360 7.8) were similar to those in the GW (4.9 and 7.6), which was consistent with the strong  
361 influence of the GW (Table 1). Given how different sample A is from all others, it appears  
362 likely that contamination or preservation issues might have occurred. Nevertheless, the pK  
363 values of sample A are listed for data completeness, but will not be used for further analysis  
364 or discussion. In tidal waters, the total concentrations of the two charge groups showed clear  
365 differences among seasons, with much higher values in summer, followed by autumn and  
366 spring (Table 1).

367

### 368 **3.4 Effects of OrgAlk on the CO<sub>2</sub> system and buffer capacity**

369

370 The impact of OrgAlk on the CO<sub>2</sub> system (i.e.  $\Delta H^+$ ,  $\Delta pCO_2$ , and  $\Delta\beta_H$  defined in section 2.4)  
371 is shown as a function of relative OrgAlk abundance (OrgAlk% in TA) and measured pH  
372 (Fig. 5). Use of relative OrgAlk abundance, rather than concentration, accounts for tidal and  
373 seasonal changes of both OrgAlk and TA. Since full titrations were only conducted on one  
374 sample for each sampling date except May 9<sup>th</sup> and October 18<sup>th</sup>, we assume that all  
375 remaining samples from the same sampling event contain similar charge groups, with the  
376 same  $pK_1$ ,  $pK_2$ , and total concentration ratios of the two charge groups (last column in Table  
377 1 and Fig. 5). The mean  $pK_1$  and  $pK_2$  values and mean total concentration ratio of the two  
378 charge groups in samples B and C were used to calculate the effects on May 9<sup>th</sup>. The  
379 samples collected on October 18<sup>th</sup> were assumed to have the same organic acid charge  
380 group characteristics as those collected on November 1<sup>st</sup>. The total concentration of each  
381 charge group in any given sample was calculated using the titrated OrgAlk concentration,  
382 the pK values, and the total concentration ratio of the two charge groups from the full  
383 titration. The ranges of  $\Delta H^+$ ,  $\Delta pCO_2$ , and  $\Delta\beta_H$  observed in tidal waters were significant given  
384 the combined uncertainties in  $\Delta H^+$ ,  $\Delta pCO_2$ , and  $\Delta\beta_H$  (Fig. 5).

385 In general, the effects of OrgAlk on H<sup>+</sup> concentrations ( $\Delta H^+$ ) ranged from 1 to 41 nmol kg<sup>-1</sup>  
386 (equivalent to a pH change of 0.03 – 0.26), increasing concurrently with the increasing  
387 OrgAlk% in TA across all three seasons at SLP (Fig. 5a). There was some seasonality in the  
388 effects of OrgAlk on H<sup>+</sup> concentrations as well. The largest effect was observed in May,  
389 coincident with the highest OrgAlk% in TA among the three seasons, subsequently  
390 decreasing in July, followed by October and November. The impact of OrgAlk on H<sup>+</sup>  
391 decreased consistently with increasing tidal water pH (Fig. 5b). In some July samples,  
392 OrgAlk increased H<sup>+</sup> concentrations considerably, but OrgAlk% in TA did not increase  
393 proportionately, highlighting that the effect of OrgAlk is influenced by both the relative  
394 OrgAlk abundance and water pH (Fig. 5a and 5b).

395 An increase of OrgAlk% in TA would generally increase  $p\text{CO}_2$  in all three seasons, showing  
396 a similar pattern as  $\Delta\text{H}^+$  (Fig. 5). The OrgAlk effect on  $p\text{CO}_2$  varied by 8 – 80% with a  
397 mean of 38% across the OrgAlk range (0.9 – 4.3% in TA) observed in this study. Relatively  
398 large effects on  $p\text{CO}_2$  occurred in May (Fig. 5c), when the relative OrgAlk abundance was  
399 generally high and sample pH was low.  $\Delta p\text{CO}_2$  was lower in July (mean  $\sim 880 \mu\text{atm}$ ) than  
400 in May (mean  $\sim 960 \mu\text{atm}$ ) and reached the lowest values in October and November (mean  
401  $\sim 200 \mu\text{atm}$ ).  $\Delta p\text{CO}_2$  increased with a decrease in pH (Fig. 5d), as more carbonate species  
402 shifted to dissolved  $\text{CO}_2$  at lower pH. The large variation of  $\Delta p\text{CO}_2$  over tidal cycles on  
403 May 25<sup>th</sup> and in July can be attributed to the large variation in pH (Fig. 5d). Compared to  
404 October and November, the higher  $\Delta p\text{CO}_2$  values at similar OrgAlk% in July may also be  
405 due to lower pH values (Fig. 5c and 5d).  
406 Compared with  $\text{H}^+$  and  $p\text{CO}_2$ , the effect of OrgAlk on the buffer capacity ( $\Delta\beta_{\text{H}}$ ) was more  
407 complex (Fig. 5e and 5f). As the proportion of OrgAlk in TA increased, its effect on  $\beta_{\text{H}}$   
408 generally changed from reducing buffer capacity (negative values) to increasing buffer  
409 capacity (positive values), and in many cases the effect was close to zero. In July and on  
410 May 25<sup>th</sup>,  $\Delta\beta_{\text{H}}$  showed both positive and negative values over the same tidal cycle, while on  
411 May 9<sup>th</sup>, OrgAlk effects were generally positive, compared with the mainly negative values  
412 in October and November. Similar to  $\Delta p\text{CO}_2$ , some samples over the same tidal cycle at  
413 similar OrgAlk% showed large variations in  $\Delta\beta_{\text{H}}$ , especially on May 25<sup>th</sup> and July 12<sup>th</sup>. Such  
414 an effect can be better illustrated in the  $\Delta\beta_{\text{H}} - \text{pH}$  plot (Fig. 5f), where there was generally a  
415 negative relationship with pH (Fig. 5f). When pH was below  $\sim 7.5$ ,  $\Delta\beta_{\text{H}}$  was generally  
416 positive, while when pH was  $> 7.5$ ,  $\Delta\beta_{\text{H}}$  became negative. This is coincident with the  
417 minimum buffer capacity of seawater occurring at  $\text{pH} \approx 7.5$ . When  $\text{pH}$  is  $> 7.5$ ,  $\text{CO}_3^{2-}$   
418 provides the main control on the buffer capacity, while when  $\text{pH}$  is  $< 7.5$ ,  $\text{HCO}_3^-$  is the  
419 principal species in control. As a result, there is a relatively large scatter in  $\Delta\beta_{\text{H}}$  at similar  
420 OrgAlk%, depending on sample pH (Fig. 5e).

421

## 422 Discussion

423

### 424 4.1 Sources of OrgAlk

425

426 Tidal creeks within salt marshes are mixing zones between coastal water, GW, and  
427 porewater flushed from the marsh during tidal exchange. Mixing of these three sources was  
428 apparent during all three seasons (Fig. 6). The coastal water OrgAlk concentration was  
429 generally lower than in waters from the salt marsh tidal creek (Fig. 6). Although coastal  
430 waters were not sampled on the same dates as the salt marsh tidal creek, we anticipate the  
431 seasonal and interannual variation of OrgAlk in Vineyard Sound to be small, given that  
432 OrgAlk concentrations in March and July were similarly low (21 and  $16 \mu\text{mol kg}^{-1}$ ,  
433 respectively) (Fig. 6). Within the tidal creek, OrgAlk concentrations increased as salinity  
434 decreased although there were considerable variations among both tidal cycles and seasons.  
435 This suggests that GW, as the main freshwater source, may be an important source of  
436 OrgAlk to the marsh-influenced tidal water.

437 The salt marsh is likely another significant OrgAlk source. The highest DOC concentrations  
438 in tidal waters appeared in July when the GW influence was relatively low (Fig. 4),  
439 implying high in-situ production in the salt marsh. OrgAlk concentrations generally  
440 increased with increasing DOC concentrations during the period of low GW influence (July  
441 26<sup>th</sup>, October, and November) (Fig. 7), an indication of OrgAlk contribution from the  
442 marsh.

443 The relative contributions of GW and marsh production to OrgAlk were assessed based on  
444 conservative mixing between the GW and coastal water end-members, and OrgAlk  
445 additions in tidal waters. The three GW samples collected from different depths were  
446 variable (177 – 485  $\mu\text{mol kg}^{-1}$ ). If the GW sample collected at shallow depth (485  $\mu\text{mol kg}^{-1}$ ,  
447 0.56 m) represented the potential GW end-member, then the tidal creek samples would fall  
448 below the mixing line between GW and Vineyard Sound waters, implying that the marsh is  
449 a significant OrgAlk sink. The marsh was a pronounced source of DOC (Fig. 4), so such an  
450 explanation is unlikely. The deep GW (177  $\mu\text{mol kg}^{-1}$ , 1.8 m) may be a more reasonable  
451 end-member. Indeed, the mixing line connecting the average values of the two Vineyard  
452 Sound waters with the GW collected at 1.8 m (dashed red line in Fig. 6) is similar to the  
453 mixing line between Vineyard Sound water and the lowest salinity tidal water sample (solid  
454 blue line in Fig. 6). The extrapolated freshwater end-member of this tidal water mixing line  
455 was 182  $\mu\text{mol kg}^{-1}$ , similar to the deep GW. Therefore, we considered the deep GW as the  
456 most representative freshwater end-member to constrain the GW OrgAlk contribution to  
457 tidal water, recognizing that the best end-member would be a flow-weighted average of GW  
458 discharging to the creek.

459 The potential GW OrgAlk contributions to tidal creek samples were calculated from sample  
460 salinity, assuming conservative mixing between coastal water and the deepest GW, while  
461 marsh contributions were assessed based on deviations above this mixing line (dashed red  
462 line in Fig. 6). Over tidal cycles in May and on July 12<sup>th</sup> when the GW influence was high,  
463 GW contributed, on average, 54% of the measured OrgAlk, much more than the average  
464 marsh contribution of 17%. In tidal water samples with limited GW influence (July 26<sup>th</sup>,  
465 October, and November), the marsh contribution accounted for 0 – 54% of OrgAlk  
466 concentrations with a mean value of 20%, compared to an average GW contribution of 31%.  
467 The greatest marsh contribution occurred on July 26<sup>th</sup>, when an estimated mean of 36% of  
468 the OrgAlk in tidal water was from the marsh, greater than the GW contribution with a  
469 mean of 24%. We further note that the concentration analysis provided here does not  
470 consider varying water flux rates across tidal cycles and variability of the GW source, which  
471 may cause potential uncertainties in this analysis.

472

## 473 **4.2 Variations of OrgAlk versus DOC**

474

475 OrgAlk showed a generally positive correlation ( $p < 0.01$ ,  $r^2 = 0.252$ ,  $n = 48$ ) with DOC in  
476 tidal creek water (Fig. 7). Nevertheless, it is apparent that some non-OrgAlk molecules in  
477 the DOC pool cycled differently from organic acid charge groups. Whereas OrgAlk samples  
478 fell along or above the conservative mixing line between deep GW and Vineyard Sound

479 coastal water (Fig. 6), almost all of the tidal creek DOC samples in May fell below it  
480 (Supplementary Data A3). It is likely that humic substances, which may be the main  
481 components of OrgAlk (Cai et al., 1998; Lukawska-Matuszewska et al., 2018), are  
482 relatively recalcitrant and thus preferentially preserved, relative to other organic molecules  
483 in the DOC pool, during GW transport and water mixing within the tidal creek.

484 The complex relationship between OrgAlk and DOC can be evaluated through  
485 OrgAlk:DOC ratios in tidal waters, GW, and Vineyard Sound coastal waters over different  
486 tides and seasons (Fig. 8). The GW samples contained high OrgAlk concentrations (Fig. 6)  
487 and very high DOC concentrations (1,500  $\mu\text{mol kg}^{-1}$  in deep GW to 7,000  $\mu\text{mol kg}^{-1}$  in  
488 shallow GW), which resulted in extremely low OrgAlk:DOC ratios ( $< 0.15$ ). The  
489 OrgAlk:DOC ratio increased with GW depth, accompanied with a three-fold OrgAlk  
490 decrease vs. a five-fold DOC decrease, which may again indicate preferential removal of  
491 some non-OrgAlk components of the DOC pool relative to organic acid charge groups  
492 along the GW flow path. In the tidal creek, OrgAlk:DOC ratios were highest in May among  
493 the three sampling seasons, when the GW influence was greatest (Fig. 8). Since GW has a  
494 low OrgAlk:DOC ratio, the plausible explanation again might be of the preferential removal  
495 of non-OrgAlk molecules in the DOC pool during GW transport and water mixing within  
496 the tidal creek. The OrgAlk:DOC ratios were lowest in July, concurrent with much higher  
497 DOC, relative to OrgAlk production in the salt marsh (Fig. 7). Coastal water and the tidal  
498 waters in October and November showed relatively high OrgAlk:DOC ratios, driven by low  
499 DOC concentrations.

500 Previous studies have used fixed organic acid to DOC ratios to estimate the abundance of  
501 OrgAlk from DOC concentrations (e.g., Morel and Hering, 1993; Hunt et al., 2011; Wang et  
502 al., 2013). Furthermore, recent studies have tried to determine the acid-base properties of  
503 DOC using a single acid-base dissociation constant and a fixed fraction of DOC (Kulinski et  
504 al., 2014; Ulfsbo et al., 2015; Hammer et al., 2017). The results from this study suggest that  
505 the OrgAlk:DOC ratio is highly variable over both time (tidal and seasonal cycle, 0.1 to  
506 0.28) and space (GW, marsh tidal and coastal waters, 0.07 to 0.28), potentially driven by  
507 various controlling factors such as DOC sources and quality, water mixing, and  
508 decomposition processes. This work as well as previous studies suggest that the sources of  
509 organic acid charge groups in coastal water include rivers, wetlands, groundwater, and  
510 phytoplankton production, all of which respond to different environmental drivers, thus  
511 altering OrgAlk:DOC ratios. Therefore, it is insufficient to account for OrgAlk contributions  
512 through DOC concentration measurements alone.

513

### 514 **4.3 Characteristics of identified charge groups**

515

516 The apparent pK values of organic acid charge groups were used to identify the  
517 characteristics of these charge groups. The first charge group had a pK<sub>1</sub> value of 4.1 to 5.5  
518 (Table 1), and likely corresponds to the carboxylic acid group (Cai et al., 1998). The  
519 carboxylic acid group is present in coastal waters and culture experiments of marine  
520 phytoplankton (Muler and Bleie, 2008; Ko et al., 2016), and considered to be a significant

521 contributor to alkalinity in natural waters (Ritchie and Perdue, 2003). GW had a  $pK_1$  value  
522 (4.9) similar to Vineyard Sound coastal water (4.9), suggesting an analogous carboxylic acid  
523 group composition. The  $pK_1$  values in the tidal creek samples with low salinity ( $S_p = 23 -$   
524  $24$ ,  $pK_1 = 5.1 - 5.5$ ) were close to that in GW, consistent with a GW source of OrgAlk in the  
525 tidal creek. In tidal water samples with higher salinity ( $S_p = 27 - 31$ ),  $pK_1$  values (4.1 – 4.6)  
526 were lower than those in the two end-members, potentially indicating influence of marsh  
527 pore water.

528 The 2<sup>nd</sup> charge group had a  $pK_2$  value of 7.4 to 8.4 (Table 1) and may match phenolic or  
529 amine species, as reported by Paxeus and Wedborg (1985) in river samples with  $pK = 8.11$ .  
530 Compared to GW ( $pK_2 = 7.6$ ), Vineyard Sound coastal water had a higher  $pK_2$  value (8.3),  
531 suggesting disparate phenolic or amine species in these waters. The  $pK_2$  values in samples B  
532 (7.4) and C (7.8) with low salinity ( $S_p = 23 - 24$ ) were similar to that in GW, while the  
533 samples collected in July and November had  $pK_2$  values (8.1 – 8.4) similar to Vineyard  
534 Sound coastal water. Thus, the characteristics of the charge groups reflect significant GW  
535 influence in the tidal creek in May, but greater contributions from both coastal water and  
536 marsh sources in July and November. The tidal creek water contained more phenolic and/or  
537 amine species than carboxylic acid groups, as shown by the higher total concentrations of  
538  $X_{2T}$  than  $X_{1T}$  (Table 1). Nonetheless, charge group 1 contributed more to TA in all seasons  
539 due to its much lower  $pK$  values, resulting in more deprotonated carboxylic acid groups in  
540 the pH range of marsh tidal water. Note that the concentration of OrgAlk should  
541 theoretically be equal to the sum of  $[X_1^-] + [X_2^-]$  (not the sum of  $X_{1T} + X_{2T}$ , since these  
542 contain both the acid and base pairs). Nevertheless, the estimated  $[X_1^-]$  and  $[X_2^-]$  for these  
543 samples did not exactly match titrated OrgAlk concentrations, likely because we ignored the  
544 effects of ionic strength when we modeled the organic acid charge groups.

545 It is worth noting that Ulfsbo et al. (2015) proposed that OrgAlk might not fit well with  
546 Dickson's definition of TA (Dickson, 1981). Dickson chose a pH endpoint of 4.5, far from  
547 the  $pK$  values of the main weak acids in seawater (i.e., carbonic acid, boric acid, sulfate,  
548 etc.), so that the dissociation-association reactions of these acids are complete at the pH  
549 endpoint. However, these results and previous studies (Cai et al., 1998; Muller and Bleie,  
550 2008; Ulfsbo et al., 2015) indicate that some organic acid charge groups might have  $pK$   
551 values near 4.5, making acid-base categorization difficult for them. In addition, the  
552 traditional Gran-type titration method used here and in many other studies is conducted in  
553 the pH range of 3.0 – 3.8. Some organic acid charge groups may be titrated in this lower pH  
554 range that would not otherwise be titrated at pH 4.5, thus causing potential bias in OrgAlk  
555 concentrations, based on the definition of TA. Nevertheless, given the uncertainty in the  $pK$   
556 values of these organic charge groups, we cannot predict whether titrated OrgAlk is biased  
557 and by how much. Future studies are warranted to address how to better include OrgAlk in  
558 the TA definition and to improve titration methods to determine OrgAlk more accurately.

559

#### 560 **4.4 Common effects of OrgAlk in different coastal waters**

561

562 Given the similarity in charge groups of organic acids in coastal waters across multiple



563 seasons and different environments, as shown in this study (section 4.3) and others, we  
564 examined whether there are any common features or differences in OrgAlk effects on  
565 carbonate chemistry across various coastal water systems. Here, we define coastal systems  
566 as the area from the upper reach of tidal water to the shelf break. We consider three  
567 idealized environments that represent typical scenarios in the northeastern U.S. coastal  
568 region: 1) offshore coastal water, 2) marsh-influenced water without any freshwater input,  
569 and 3) estuarine water, where offshore coastal water mixes with a freshwater source rich in  
570 OrgAlk, such as river water or GW. In each case, the characteristics of salinity, temperature,  
571 TA, DIC, and OrgAlk were set at representative values of these coastal environments as  
572 observed in this study (Table 2). The effects of OrgAlk on the CO<sub>2</sub> system speciation and  
573 buffer capacity ( $\Delta H^+$ ,  $\Delta pCO_2$ , and  $\Delta\beta_H$ ) were estimated as discussed in section 3.4 by  
574 varying  $X_{1T}$  and  $X_{2T}$  concentrations, thus changing OrgAlk% in TA, but keeping the  
575  $X_{2T}/X_{1T}$  and pK values of charge groups constant (Fig. 9).

576 For all three cases, as the OrgAlk relative contribution to TA increases, its effect on the H<sup>+</sup>  
577 concentration increases (Fig. 9a), while the magnitude is somewhat different for each case.  
578 Marsh-influenced water (case 2) shows the greatest sensitivity to increasing proportion of  
579 OrgAlk, followed by estuarine water (case 3) and offshore coastal water (case 1). The main  
580 reason for the different sensitivity of  $\Delta H^+$  to OrgAlk% in TA are the specific DIC and TA  
581 conditions of each of the three cases that result in different water pH and buffer capacity.  
582 Compared to offshore coastal water, estuarine water and marsh-influenced water have lower  
583 buffer capacities, as their initial pH values are near 7.5. Lower pH in marsh-influenced  
584 water leads to a greater change in H<sup>+</sup> concentration with OrgAlk addition, compared to the  
585 other two cases. Nevertheless, the magnitude of the effect of OrgAlk on H<sup>+</sup> concentration is  
586 significant for all three cases of coastal environments, with the largest H<sup>+</sup> concentration  
587 increase of 8 – 41 nmol kg<sup>-1</sup> (equivalent to a pH change of 0.23 – 0.27) in the OrgAlk  
588 proportion range (0.9 – 4.3%) observed in this study.

589 Similar to H<sup>+</sup> concentration, the impact of OrgAlk on  $pCO_2$  increases with the relative  
590 abundance of OrgAlk in the three coastal waters (Fig. 9b). The impact on  $pCO_2$  is more  
591 pronounced for marsh-influenced water and estuarine water than for offshore coastal water  
592 mainly because of the difference in their buffer capacity. Dissolved CO<sub>2</sub>, thus  $pCO_2$ , of  
593 offshore coastal water increases slowly as a result of CO<sub>3</sub><sup>2-</sup> buffering until most of CO<sub>3</sub><sup>2-</sup> is  
594 consumed and the water shifts to a HCO<sub>3</sub><sup>-</sup> buffer system (Fig. 9b). In contrast, both  
595 marsh-influenced water and estuarine water have an initial pH near 7.5, so less CO<sub>3</sub><sup>2-</sup> exists  
596 to buffer against increased dissolved CO<sub>2</sub> in the system. Therefore, in the more acidic  
597 coastal environments, such as tidal marshes and freshwater-influenced estuaries, the effect  
598 of OrgAlk on  $pCO_2$ , and thus CO<sub>2</sub> fluxes, is expected to be greater than in offshore water. It  
599 is worth noting that OrgAlk influences  $pCO_2$  values by changing water pH thus the  
600 speciation of carbonic acid in natural waters. Using measured pH and DIC as the input pair  
601 to calculate  $pCO_2$  values accounts for the effect of OrgAlk, resulting in a much smaller  
602  $pCO_2$  calculation error. Using pH and TA as the input pair, without correcting the latter for  
603 OrgAlk, is equivalent to treating OrgAlk as carbonate alkalinity in TA. This will  
604 overestimate DIC and  $pCO_2$  values in carbonic acid speciation calculations. Lastly, using

605 the TA-DIC pair without accounting for OrgAlk will result in underestimation of  $p\text{CO}_2$   
606 values, as shown in this study.

607 OrgAlk affects  $\beta_{\text{H}}$  for the three coastal water cases, similarly to  $p\text{CO}_2$  (Fig. 9c). As the  
608 relative OrgAlk proportion increases in offshore coastal waters, lowering pH,  $\beta_{\text{H}}$  decreases  
609 (i.e., negative  $\Delta\beta_{\text{H}}$ ) until pH decreases to  $\sim 7.5$  (the case 1 curve becomes flat in Fig. 9c).  
610 On the other hand, both marsh and estuarine waters are already  $\text{HCO}_3^-$  buffer systems, and  
611 thus increasing OrgAlk% increases  $\text{HCO}_3^-$  concentration, and thus  $\beta_{\text{H}}$  (positive  $\Delta\beta_{\text{H}}$ ).

612

### 613 **A conceptual coastal OrgAlk model**

614

615 This study has systematically investigated the contributions of organic acid charge groups in  
616 the DOC pool to TA and estimated the impact of OrgAlk on the  $\text{CO}_2$  system in salt marsh-  
617 and groundwater-influenced coastal water for the first time. The high concentrations of  
618 OrgAlk observed in marsh tidal water have an important effect on water pH, carbonate  
619 speciation, and thus  $\text{CO}_2$  fluxes. To summarize, we present a conceptual model of OrgAlk  
620 sources and sinks within the coastal ocean (Fig. 10) based on the findings from this and  
621 previous studies (Kieber et al., 1990; Lovley et al., 1996; Cai et al., 1998; Uyguner and  
622 Bekbolet, 2005; Hernández-Ayon et al., 2007; Muller and Bleie, 2008; Kim and Lee, 2009;  
623 Wang et al., 2013; Ko et al., 2016; Hammer et al., 2017; Lukawska-Matuszewska et al.,  
624 2018). Traditionally, DOC contributes to the DIC pool through microbial remineralization,  
625 generating  $\text{CO}_2$  and alkalinity (mostly by anaerobic pathways), and by photodegradation. In  
626 the conceptual model shown here, the organic acid charge groups of the DOC pool directly  
627 contribute alkalinity (OrgAlk), providing a biogeochemical link between the DOC and DIC  
628 pools in the coastal ocean by partially regulating pH, and thus  $p\text{CO}_2$  and buffer capacity  
629 (Fig. 10).

630 In coastal environments where OrgAlk concentrations may be high, it is important to  
631 consider the effect of OrgAlk on the  $\text{CO}_2$  system and carbon fluxes. As the composition of  
632 organic acid charge groups are inherently complex, the modeling method used in this and  
633 other studies (i.e. Eq. (2)) still lacks the ability to discern charge groups of organic acids  
634 across coastal waters with different ionic strengths. The model by Ulfsbo et al. (2015) might  
635 facilitate explicit understanding of the composition of organic acid charge groups in marine  
636 environments since it combines a humic ion binding model with an ionic interaction model.  
637 In general, we have a limited understanding of the generation and removal pathways of  
638 organic acid charge groups, their composition, and biogeochemical role in coastal waters  
639 and beyond. Thus, future studies are warranted to improve our understanding of organic  
640 acid charge groups in order to better quantify the linkage between organic and inorganic  
641 carbon cycling.

642

643 **Acknowledgements**

644

645 We thank the associate editor Alfonso Mucci and three anonymous reviewers for their  
646 insightful comments, which improved the manuscript significantly. We thank Kate  
647 Morkeski, Lloyd Anderson, Zoe Sandwith, Xiao-bo Ni, Mallory Ringham, Eyal Wurgaft,  
648 Wei-jun Cai, Wen-yun Guo, and Ai-mei Wang for sampling, analytical, and modeling  
649 assistance; USGS staff including T. Wallace Brooks, Jennifer O’Keefe Suttles, Adrian Mann  
650 for field and analytical support; Jordan Mora and other staff at the Waquoit Bay NERR for  
651 sampling, analysis, and mapping support. The study was supported by the USGS Coastal &  
652 Marine Geology Program, the USGS Land Change Science Program’s LandCarbon  
653 program, the U.S. National Science Foundation (OCE-1459521), the NOAA Science  
654 Collaborative program (NA09NOS4190153), and the China Scholarship Council. Any use  
655 of trade, firm or product names is for descriptive purposes only and does not imply  
656 endorsement by the U.S. Government.

657

658 **References**

659

660 Abril G., Bouillon S., Darchambeau F., Teodoru C. R., Marwick T. R., Tamooch F., Ochieng  
661 O. F., Geeraert N., Deirmendjian L., Polsenaeere P. and Borges A. V. (2015) Technical Note:  
662 Large overestimation of  $p\text{CO}_2$  calculated from pH and alkalinity in acidic, organic-rich  
663 freshwaters. *Biogeosciences* **12**, 67–78.

664 Bauer J. E., Cai W. J., Raymond P. A., Bianchi T. S., Hopkinson C. S. and Regnier P. A. G.  
665 (2013) The changing carbon cycle of the coastal ocean. *Nature* **504**, 61–70.

666 Butman D. and Raymond P. A. (2011) Significant efflux of carbon dioxide from streams  
667 and rivers in the United States. *Nature Geosci.* **4**, 839–842.

668 Cai W. J. (2011) Estuarine and coastal ocean carbon paradox:  $\text{CO}_2$  sinks or sites of  
669 terrestrial carbon incineration? *Ann. Rev. Mar. Sci.* **3**, 123–145.

670 Cai W. J. and Wang Y. (1998) The chemistry, fluxes, and sources of carbon dioxide in the  
671 estuarine waters of the Satilla and Altamaha Rivers, Georgia. *Limnol. Oceanogr.* **43**,  
672 657–668.

673 Cai W. J., Wang Y. and Hodson R. E. (1998) Acid-base properties of dissolved organic  
674 matter in the estuarine waters of Georgia, USA. *Geochim. Cosmochim. Acta* **62**, 473–483.

675 Cambareri T. C. and Eichner E. M. (1998) Watershed delineation and ground water  
676 discharge to a coastal embayment. *Groundwater* **36**, 626–634.

677 Chu S. N., Wang Z. A., Gonneea M. E., Kroeger K. D. and Ganju N. K. (2018) Deciphering  
678 the dynamics of inorganic carbon export from intertidal salt marshes using high-frequency  
679 measurements. *Mar. Chem.* **206**, 7–18.

680 Dickson A. G. (1981) An exact definition of total alkalinity and a procedure for the  
681 estimation of alkalinity and total inorganic carbon from titration data. *Deep Sea Res. Part A.*  
682 *Oceanogr. Res. Pap.* **28**, 609–623.

683 Dickson A. G. (1990a) Thermodynamics of the dissociation of boric acid in synthetic  
684 seawater from 273.15 to 318.15 K. *Deep Sea Res. Part A. Oceanogr. Res. Pap.* **37**,  
685 755–766.

686 Dickson A. G. (1990b) Standard potential of the reaction:  $\text{AgCl (s)} + 12\text{H}_2 \text{(g)} = \text{Ag (s)} +$   
687  $\text{HCl (aq)}$ , and the standard acidity constant of the ion  $\text{HSO}_4^-$  in synthetic sea water from  
688 273.15 to 318.15 K. *J. Chem. Thermodyn.* **22**, 113–127.

689 Dickson A. G. and Riley J. P. (1979) The estimation of acid dissociation constants in  
690 seawater media from potentiometric titrations with strong base. I. The ionic product of  
691 water— $K_w$ . *Mar. Chem.* **7**, 89–99.

692 Dickson A. G., Sabine C. L. and Christian J. R. (2007) *Guide to best practices for ocean*  
693  *$\text{CO}_2$  measurements*. North Pacific Marine Science Organization, pp. 33–39.

694 Dinauer A. and Mucci A. (2017) Spatial variability in surface-water  $p\text{CO}_2$  and gas exchange  
695 in the world's largest semi-enclosed estuarine system: St. Lawrence Estuary  
696 (Canada). *Biogeosciences* **14**, 3221–3237.

697 Douglas N. K. and Byrne R. H. (2017) Spectrophotometric pH measurements from river to  
698 sea: Calibration of mCP for  $0 \leq S \leq 40$  and  $278.15 \leq T \leq 308.15$  K. *Mar. Chem.* **197**,

699 64–69.

700 Downing B. D., Boss E., Bergamaschi B. A., Fleck J. A., Lionberger M. A., Ganju N. K.,  
701 Schoellhamer D. H. and Fujii R. (2009) Quantifying fluxes and characterizing  
702 compositional changes of dissolved organic matter in aquatic systems in situ using  
703 combined acoustic and optical measurements. *Limnol. Oceanogr. Methods* **7**, 119–131.

704 Egleston E. S., Sabine C. L. and Morel F. M. M. (2010) Revelle revisited: Buffer factors  
705 that quantify the response of ocean chemistry to changes in DIC and alkalinity. *Global*  
706 *Biogeochem. Cycles* **24**, 1–9.

707 Garcia-Mina J. M. (2006) Stability, solubility and maximum metal binding capacity in  
708 metal–humic complexes involving humic substances extracted from peat and organic  
709 compost. *Org. Geochem.* **37**, 1960–1972.

710 Hammer K., Schneider B., Kuliński K. and Schulz-Bull D. E. (2017) Acid-base properties  
711 of Baltic Sea dissolved organic matter. *J. Mar. Syst.* **173**, 114–121.

712 Hernández-Ayon J. M., Zirino A., Dickson A. G., Camiro-Vargas T. and  
713 Valenzuela-Espinoza E. (2007) Estimating the contribution of organic bases from  
714 microalgae to the titration alkalinity in coastal seawaters. *Limnol. Oceanogr. Methods* **5**,  
715 225–232.

716 Holmquist J. R., Windham-Myers L., Bliss N., Crooks S., Morris J. T., Megonigal P. J.,  
717 Troxler T., Weller D., Callaway J., Drexler J., Ferner M. C., Gonnee M. E., Kroeger K. D.,  
718 Schile-Beers L., Woo I., Buffington K., Boyd B. M., Breithaupt J., Brown L. N., Dix N.,  
719 Hice L., Horton B. P., MacDonald G. M., Moyer R. P., Reay W., Shaw T., Smith E., Smoak J.  
720 M., Sommerfield C., Thorne K., Velinsky D., Watson E., Grimes K. W. and Woodrey M.  
721 (2018) Accuracy and Precision of Tidal Wetland Soil Carbon Mapping in the Conterminous  
722 United States. *Sci. Rep.* **8**, 9478.

723 Hunt C. W., Salisbury J. E. and Vandemark D. (2011) Contribution of non-carbonate anions  
724 to total alkalinity and overestimation of  $p\text{CO}_2$  in New England and New Brunswick rivers.  
725 *Biogeosciences* **8**, 3069–3076.

726 Kaltin S. and Anderson L. G. (2005) Uptake of atmospheric carbon dioxide in Arctic shelf  
727 seas: evaluation of the relative importance of processes that influence  $p\text{CO}_2$  in water  
728 transported over the Bering–Chukchi Sea shelf. *Mar. Chem.* **94**, 67–79.

729 Kieber R. J., Zhou X. and Mopper K. (1990) Formation of carbonyl compounds from  
730 UV-induced photodegradation of humic substances in natural waters: Fate of riverine  
731 carbon in the sea. *Limnol. Oceanogr.* **35**, 1503–1515.

732 Kim H. and Lee K. (2009) Significant contribution of dissolved organic matter to seawater  
733 alkalinity. *Geophys. Res. Lett.* **36**, L20603.

734 Ko Y. H., Lee K., Eom K. H. and Han I. (2016) Organic alkalinity produced by  
735 phytoplankton and its effect on the computation of ocean carbon parameters. *Limnol.*  
736 *Oceanogr.* **61**, 1462–1471.

737 Koeve W. and Oschlies A. (2012) Potential impact of DOM accumulation on  $f\text{CO}_2$  and  
738 carbonate ion computations in ocean acidification experiments. *Biogeosciences* **9**,  
739 3787–3798.

740 Kuliński K., Schneider B., Hammer K., Machulik U. and Schulz-Bull D. (2014) The

741 influence of dissolved organic matter on the acid–base system of the Baltic Sea. *J. Mar. Syst.*  
742 **132**, 106–115.

743 Lee K., Kim T. W., Byrne R. H., Millero F. J., Feely R. A. and Liu Y. M. (2010) The  
744 universal ratio of boron to chlorinity for the North Pacific and North Atlantic  
745 oceans. *Geochim. Cosmochim. Acta* **74**, 1801–1811.

746 Lovley D. R., Coates J. D., Blunt-Harris E. L., Phillips E. J. P. and Woodward J. C. (1996)  
747 Humic substances as electron acceptors for microbial respiration. *Nature* **382**, 445–448.

748 Lukawska-Matuszewska K., Grzybowski W., Szewczun A. and Tarasiewicz P. (2018)  
749 Constituents of organic alkalinity in pore water of marine sediments. *Mar. Chem.* **200**,  
750 22–32.

751 Mann A. G., Kroeger K. D., O’Keefe Suttles J. A., Gonneea M. E., Brosnahan S. B. and  
752 Brooks T. W. (2019) Time-series of biogeochemical and flow data from a tidal salt-marsh  
753 creek, Sage Lot Pond, Waquoit Bay, Massachusetts (2012-2016), U.S. Geological Survey  
754 data release, <https://doi.org/10.5066/P9STIROQ>.

755 Masini J. C., Abate G., Lima E. C., Hahn L. C., Nakamura M. S., Lichtig J. and Nagatomy  
756 H. R. (1998) Comparison of methodologies for determination of carboxylic and phenolic  
757 groups in humic acids. *Anal. Chim. Acta* **364**, 223–233.

758 Morel F. M. M. and Hering J. G. (1993) *Principles and Applications of Aquatic Chemistry*.  
759 John Wiley & Sons Inc., New York.

760 Moseman-Valtierra S., Abdul-Aziz O. I., Tang J., Ishtiaq K. S., Morkeski K., Mora J.,  
761 Quinn R. K., Martin R. M., Egan K., Brannon E. Q., Carey J. and Kroeger K. D. (2016)  
762 Carbon dioxide fluxes reflect plant zonation and belowground biomass in a coastal marsh.  
763 *Ecosphere* **7**, 1–21.

764 Muller F. L. L. and Bleie B. (2008) Estimating the organic acid contribution to coastal  
765 seawater alkalinity by potentiometric titrations in a closed cell. *Anal. Chim. Acta* **619**,  
766 183–191.

767 Najjar R. G., Herrmann M., Alexander R., Boyer E. W., Burdige D. J., Butman D., Cai W. J.,  
768 Canuel E. A., Chen R. F., Friedrichs M. A. M., Feagin R. A., Griffith P. C., Hinson A. L.,  
769 Holmquist J. R., Hu X., Kemp W. M., Kroeger K. D., Mannino A., McCallister S. L.,  
770 McGillis W. R., Mulholland M. R., Pilskaln C. H., Salisbury J., Signorini S. R., St-Laurent  
771 P., Tian H., Tzortziou M., Vlahos P., Wang Z. A. and Zimmerman R. C. (2018) Carbon  
772 budget of tidal wetlands, estuaries, and shelf waters of eastern North America. *Global*  
773 *Biogeochem. Cycles* **32**, 389–416.

774 Orr J. C., Epitalon J. M., Dickson A. G. and Gattuso J. P. (2018) Routine uncertainty  
775 propagation for the marine carbon dioxide system. *Mar. Chem.* **207**, 84–107.

776 Ouyang X. and Lee S. Y. (2014) Updated estimates of carbon accumulation rates in coastal  
777 marsh sediments. *Biogeosciences* **11**, 5057–5071.

778 Paquay F. S., Macenzie F. T. and Borges A. V. (2007) Carbon dioxide dynamics in rivers  
779 and coastal waters of the “big island” of Hawaii, USA, during baseline and heavy rain  
780 conditions. *Aquat. Geochem.* **13**, 1–18.

781 Paxeus N. and Wedborg M. (1985) Acid-base properties of aquatic fulvic acid. *Anal. Chim.*  
782 *Acta* **169**, 87–98.

783 Raymond P. A., Bauer J. E. and Cole J. J. (2000) Atmospheric CO<sub>2</sub> evasion, dissolved  
784 inorganic carbon production, and net heterotrophy in the York River estuary. *Limnol.*  
785 *Oceanogr.* **45**, 1707–1717.

786 Ritchie J. D. and Perdue E. M. (2003) Proton-binding study of standard and reference fulvic  
787 acids, humic acids, and natural organic matter. *Geochim. Cosmochim. Acta* **67**, 85–96.

788 Shi Z., Wang P., Peng L., Lin Z. and Dang Z. (2016) Kinetics of heavy metal dissociation  
789 from natural organic matter: Roles of the carboxylic and phenolic  
790 sites. *Environ. Sci. Technol.* **50**, 10476–10484.

791 Tishchenko P. Y., Wallmann K., Vasilevskaya N. A., Volkova T. I., Zvalinskii V. I.,  
792 Khodorenko N. D. and Shkirnikova E. M. (2006) The contribution of organic matter to the  
793 alkaline reserve of natural waters. *Oceanology* **46**, 192–199.

794 Ulfsbo A., Kuliński K., Anderson L. G. and Turner D. R. (2015) Modelling organic  
795 alkalinity in the Baltic Sea using a Humic-Pitzer approach. *Mar. Chem.* **168**, 18–26.

796 Uyguner C. S. and Bekbolet M. (2005) Evaluation of humic acid photocatalytic degradation  
797 by UV–vis and fluorescence spectroscopy. *Catal. Today* **101**, 267–274.

798 van Heuven S., Pierrot D., Rae J. W. B., Lewis E. and Wallace D. W. R. (2011) MATLAB  
799 Program Developed for CO<sub>2</sub> System Calculations. ORNL/CDIAC-105b.

800 Wang Z. A. and Cai W. J. (2004) Carbon dioxide degassing and inorganic carbon export  
801 from a marsh-dominated estuary (the Duplin River): A marsh CO<sub>2</sub> pump. *Limnol. Oceanogr.*  
802 **49**, 341–354.

803 Wang Z. A., Wanninkhof R., Cai W. J., Byrne R. H., Hu X., Peng T. H. and Huang W. J.  
804 (2013) The marine inorganic carbon system along the Gulf of Mexico and Atlantic coasts of  
805 the United States: Insights from a transregional coastal carbon study. *Limnol. Oceanogr.* **58**,  
806 325–342.

807 Wang Z. A., Kroeger K. D., Ganju N. K., Gonneea M. E. and Chu S. N. (2016) Intertidal  
808 salt marshes as an important source of inorganic carbon to the coastal ocean. *Limnol.*  
809 *Oceanogr.* **61**, 1916–1931.

810 Yang B., Byrne R. H. and Lindemuth M. (2015) Contributions of organic alkalinity to total  
811 alkalinity in coastal waters: A spectrophotometric approach. *Mar. Chem.* **176**, 199–207.

812

813 **Figure Captions**

814

815 **Fig. 1.** Study sites. **(a)** The location of the study area in Massachusetts, USA. Water samples  
816 were collected in Waquoit Bay (red square) and Vineyard Sound (orange square); **(b)** Land  
817 use cover map of the Waquoit Bay watershed; **(c)** Salt marsh habitat map of Sage Lot Pond;  
818 **(d)** The location of sampling sites. Tidal creek water samples were collected at sampling site  
819 1. Ground water (GW) samples were collected at sampling site 2. Maps **(b)** and **(c)** are  
820 courtesy of Jordan Mora, Waquoit Bay National Estuarine Research Reserve.

821

822 **Fig. 2.** **(a)** Flow chart of OrgAlk titration; **(b)** Schematic of the OrgAlk titration equipment:  
823 (1) and (2) KloeHN digital syringe pumps; (3) NaOH solution; (4) HCl solution; (5) Water  
824 bath; (6) Magnetic stir; (7) Stir bar; (8) pH electrode; (9) Titration vessel with sample; (10)  
825 pH meter; (11) Computer; (12) Soda lime plug.

826

827 **Fig. 3.** Comparison between titrated OrgAlk concentrations and excess alkalinity ( $\Delta TA$ )  
828 calculated as the difference between measured TA ( $TA_{mea}$ ) and calculated TA ( $TA_{cal}$ ) using  
829 measured DIC-pH as the input pair at Sage Lot Pond in May, July, October, and November  
830 2016. The dashed line is a 1:1 line indicating where titrated OrgAlk concentrations are equal  
831 to excess alkalinity.

832

833 **Fig. 4.** Variations of TA, OrgAlk,  $pH_{tot}$  (pH on the total proton concentration scale at in-situ  
834 temperature), salinity, DOC, temperature, and water elevation (NAVD88) over tidal cycles  
835 in May **(a, b)**, July **(c, d)**, October **(e)**, and November **(f)** 2016 at Sage Lot Pond. The scales  
836 for each parameter are consistent across plots for convenience of comparison.

837

838 **Fig. 5.** The effects of OrgAlk on  $H^+$ ,  $pCO_2$ , and buffer capacity ( $\beta_H$ ) over three seasons at  
839 Sage Lot Pond.  $\Delta H^+$ ,  $\Delta pCO_2$ , and  $\Delta \beta_H$  represent the differences in  $H^+$ ,  $pCO_2$ , and  $\beta_H$   
840 between the values calculated by including OrgAlk and those without, using measured TA  
841 and DIC as input pair. **(a)**, **(c)**, and **(e)** show  $\Delta H^+$ ,  $\Delta pCO_2$ , and  $\Delta \beta_H$  variations with OrgAlk%  
842 in TA in May, July, October, and November 2016. **(b)**, **(d)**, and **(f)** show the changes of  $\Delta H^+$ ,  
843  $\Delta pCO_2$ , and  $\Delta \beta_H$  as a function of measured pH. The vertical bars for data points indicate the  
844 uncertainties in  $\Delta H^+$ ,  $\Delta pCO_2$ , and  $\Delta \beta_H$ , respectively.

845

846 **Fig. 6.** Variations of OrgAlk concentrations with salinity in tidal water at Sage Lot Pond  
847 (SLP) in May, July, October, and November 2016. The purple stars in the inset represent  
848 OrgAlk concentrations in GW collected at the edge of the SLP marsh (41.55443N,  
849 70.5054W; Fig. 1). The yellow and blue stars at high salinity represent OrgAlk  
850 concentrations in coastal water of Vineyard Sound (VS) off SLP. The dashed red line is the  
851 mixing line between Vineyard Sound water and GW at depth of 1.8 m. The solid blue line is  
852 the mixing line between Vineyard Sound water and the lowest salinity SLP tidal water.

853

854 **Fig. 7.** Variations of OrgAlk and DOC concentrations in tidal creek water at SLP in May,



855 July, October, and November 2016. The purple stars in the inset show OrgAlk and DOC  
856 concentrations in GW collected at the edge of the SLP marsh. The blue star represents  
857 OrgAlk and DOC concentrations in Vineyard Sound coastal water (VS) off SLP. The black  
858 line indicates the linear correlation between DOC and OrgAlk concentrations ( $p < 0.01$ ,  $r^2 =$   
859  $0.252$ ,  $n = 48$ ).

860

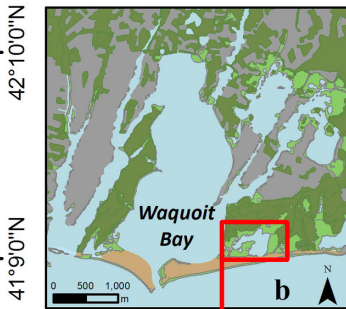
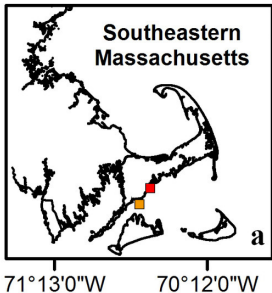
861 **Fig. 8.** Variations of OrgAlk:DOC ratios with salinity in tidal water at Sage Lot Pond in  
862 May, July, October, and November 2016, and in GW and Vineyard Sound coastal water  
863 end-members.

864

865 **Fig. 9.** Effects of OrgAlk on  $H^+$  (a),  $pCO_2$  (b), and  $\beta_H$  (c) in three cases of coastal waters.  
866  $\Delta H^+$ ,  $\Delta pCO_2$ , and  $\Delta \beta_H$  were calculated similarly as in Fig. 5 (also see section 3.4). The color  
867 bands around each solid line of three cases of coastal waters indicate the uncertainties in  
868  $\Delta H^+$ ,  $\Delta pCO_2$ , and  $\Delta \beta_H$ .

869

870 **Fig. 10.** A conceptual model of OrgAlk cycling in coastal systems. Alk indicates alkalinity.  
871 BioP and ChemP represent in-situ biological production and chemical production of organic  
872 acid charge groups, respectively. Boxes with dashed lines indicate processes that were not  
873 studied in the present study. The values in the boxes of pH,  $pCO_2$ , and buffer capacity ( $\beta_H$ )  
874 represent the magnitude of OrgAlk effects on pH,  $pCO_2$ , and  $\beta_H$  in the range of OrgAlk% in  
875 TA observed in this study (0.9 – 4.3%) in coastal waters.

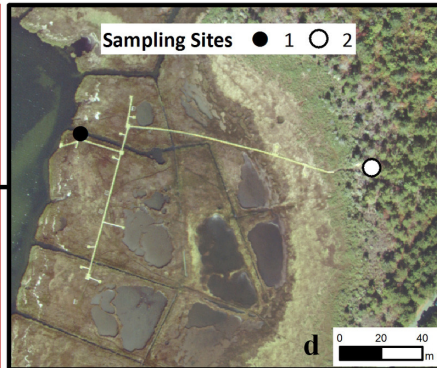
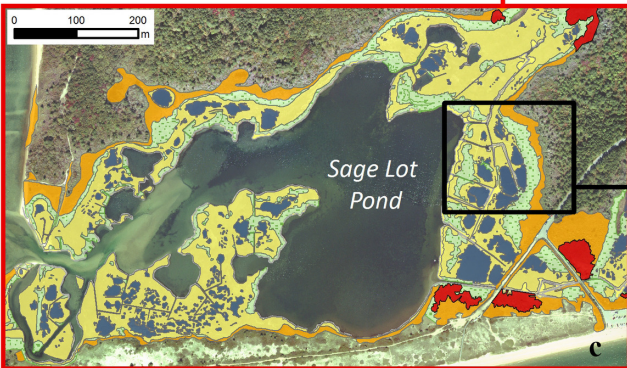


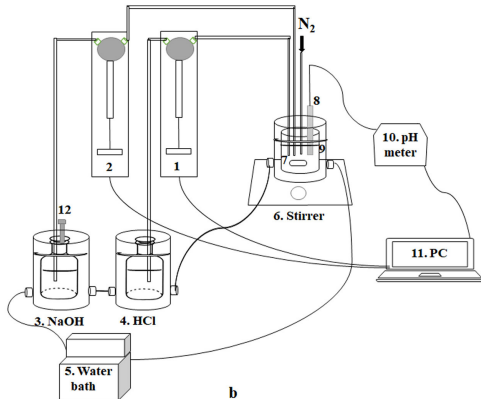
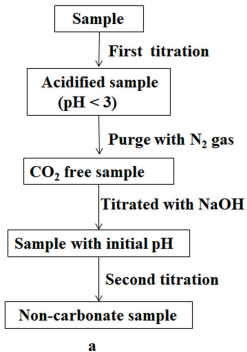
**Land Use Cover**

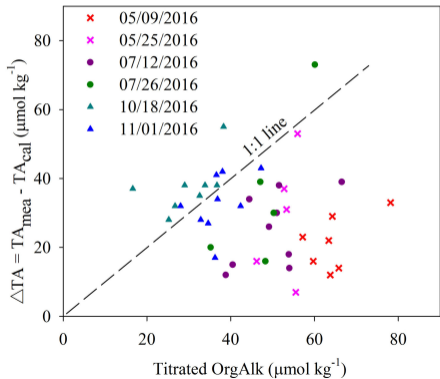
- Residential Development
- Dune Habitat
- Forested Area
- Wetland
- Open Water

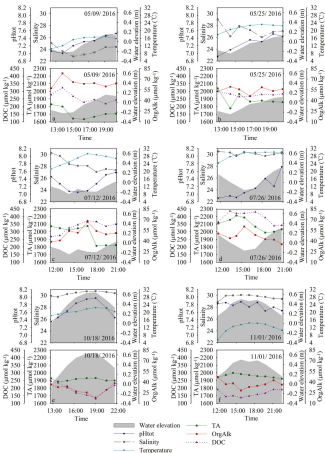
**Salt Marsh Habitats**

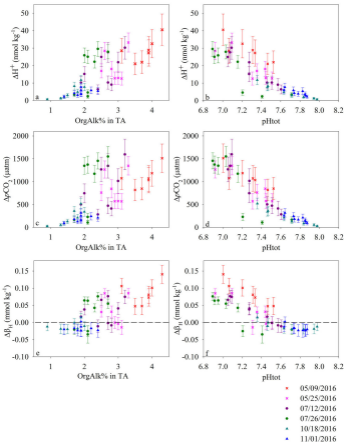
- Low Marsh
- High Marsh
- Pools
- Marsh Border
- Phragmites australis*

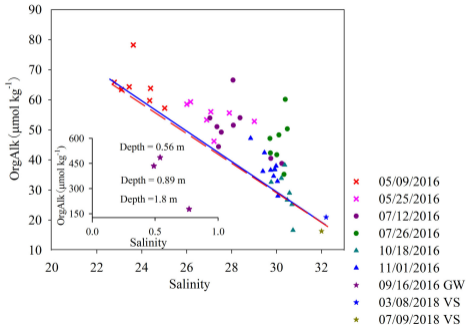


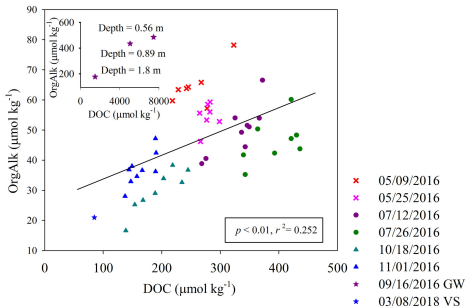




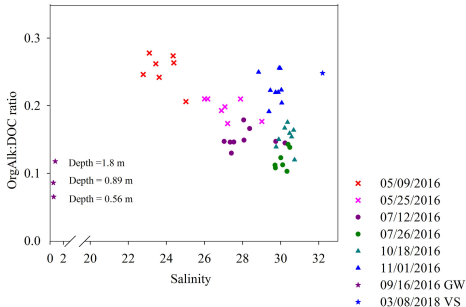


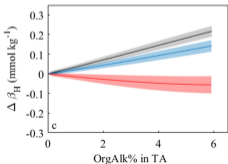
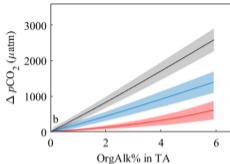
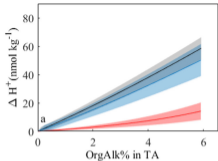












- Case 1: Offshore coastal water
- Case 2: Marsh-influenced water
- Case 3: Estuarine water

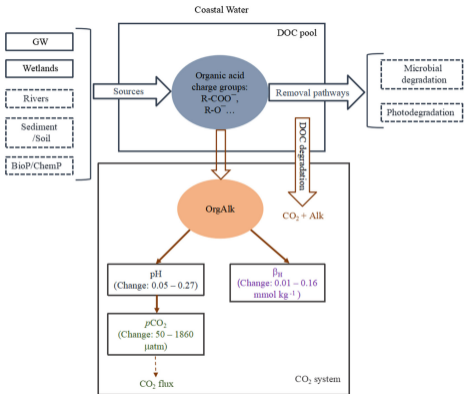


**Table 1.** Summary of full-titration of the samples collected in the study.  $pK_1$  and  $pK_2$  represent the modeled  $pK$  values of identified organic acid charge group 1 and charge group 2.  $X_{1T}$  and  $X_{2T}$  are the estimated total concentrations of charge group 1 and charge group 2, respectively. GW and VS represent groundwater and Vineyard Sound coastal water, respectively.

Sample	Collecting date	Salinity	pH	Titrated OrgAlk ( $\mu\text{mol kg}^{-1}$ )	$pK_1$	$pK_2$	$X_{1T}$ ( $\mu\text{mol kg}^{-1}$ )	$X_{2T}$ ( $\mu\text{mol kg}^{-1}$ )	$X_{2T}/X_{1T}$
A	2016.5.9	22.8	7.20	66	5.0	9.8	35	14	0.4
B	2016.5.9	23.6	7.00	78	5.5	7.4	21	33	1.6
C	2016.5.9	23.4	7.33	64	5.1	7.8	24	33	1.4
D	2016.5.25	29.0	6.92	53	4.1	7.9	62	89	1.4
E	2016.7.12	27.0	7.28	54	4.4	8.1	100	258	2.6
F	2016.7.26	30.3	7.71	35	4.2	8.4	117	301	2.6
G	2016.11.1	28.8	7.83	47	4.6	8.4	104	236	2.3
GW	2016.9.16	0.5	6.66	435	4.9	7.6	221	316	1.4
VS	2018.7.9	32.0	7.87	16	4.9	8.3	36	92	2.6

**Table 2.** Input parameters and OrgAlk characteristics used in CO2SYS calculations in three coastal water environments. The OrgAlk characteristics in offshore coastal water and marsh-influenced water were similar to the Vineyard Sound water sample and the low pH sample D in Table 1, respectively. The OrgAlk characteristic in estuarine water was based on the mean  $pK_1$ ,  $pK_2$ , and  $X_{2T}/X_{1T}$  values between samples B and C in Table 1.

	Salinity	Temperature (°C)	TA ( $\mu\text{mol kg}^{-1}$ )	DIC ( $\mu\text{mol kg}^{-1}$ )	$pK_1$	$pK_2$	$X_{2T}/X_{1T}$
<b>Offshore coastal water</b>	32.0	10	2100	1950	4.9	8.3	2.6
<b>Marsh-influenced water</b>	32.0	10	2200	2300	4.1	7.9	1.4
<b>Estuarine water</b>	20	10	1320	1360	5.2	7.6	1.5